

## VIBRATION ANALYSIS OF INDUCTION MOTOR FOR BEARING FAULTS DETECTION USING ESPRIT METHOD

### ANALIZA VIBRACIJA INDUKCIONOG MOTORA RADI DETEKCIJE OŠTEĆENJA LEŽIŠTA PRIMENOM METODE ESPRIT

Originalni naučni rad /Original scientific paper

Rad primljen / Paper received: 05.05.2024

<https://doi.org/10.69644/ivk-2025-01-0141>

Adresa autora / Author's address:

<sup>1)</sup> Faculty of Technology, Hassiba Benbouali University, Chlef, Algeria K. Azouzi <https://orcid.org/0000-0003-0279-3123>

<sup>2)</sup> Faculty of Applied Sciences, Ibn Khaldoun University, Tiaret, Algeria M. Kouadria <https://orcid.org/0000-0001-8628-9754>

<sup>3)</sup> University of Sciences and Technology, Oran, Algeria

<sup>4)</sup> Hassiba Benbouali University of Chlef, Algeria

M. Hadj Meliani <https://orcid.org/0000-0003-1375-762X>

\*email: [m.hadjmeliani@univ-chlef.dz](mailto:m.hadjmeliani@univ-chlef.dz)

#### Keywords

- vibration
- ESPRIT
- bearing faults
- induction motor
- diagnosis

#### Abstract

*The monitoring of vibrations in rotating machinery aims to provide information on the operational state of the machine without interrupting the production line. This prevents production losses and enhances reliability and safety. In this regard, this article presents a study integrated within the context of applying condition-based maintenance through vibration analysis of bearings, utilising the Estimation of Signal Parameters via Rotational Invariance Technique (ESPRIT) method to detect bearing faults in the induction motor. The results of experimental tests conducted on a 3 kW, 50 Hz induction motor demonstrate the effectiveness of the ESPRIT method in identifying low-amplitude harmonics that characterise bearing failures.*

#### INTRODUCTIONS

Ball bearings constitute a fundamental component of all electric motors, playing a crucial role as an electromechanical interface. Unfortunately, this function renders them more susceptible, placing them at the forefront of the primary causes of failure in electrical machines, /1, 2/. Among the most significant factors contributing to bearing failures, one can cite excessive load, lubricant contamination, as well as electrical issues such as the circulation of leakage currents induced by pulse-width modulation inverters (PWM), /3-6/. Indeed, statistical studies reveal that bearing defects account for between 40 % and 52 % of total motor failures in certain industrial sectors /7, 8/. This type of failure typically results in various mechanical effects within the machine, such as an increase in noise levels and the emergence of vibrations /9/. The critical point of bearing failure is manifested by the rotor locking. Therefore, it becomes imperative to detect such failures early on to ensure personnel safety and prevent production line interruptions, thereby minimising economic losses.

Vibration monitoring of electric motors is widely employed in the industry to detect various defects affecting electrical machines, with a particular focus on mechanical

#### Ključne reči

- vibracija
- ESPRIT
- oštećenja ležišta
- indukcion motor
- dijagnostika

#### Izvod

*Praćenjem vibracija kod rotacionih mašina omogućava se dobijanje informacija o operativnom stanju mašine bez prekida rada. Ovim se izbegavaju gubici u proizvodnji i poboljšava se pouzdanost i bezbednost. Imajući to u vidu, u ovom radu je predstavljeno istraživanje koje integriše kontekst primene održavanja na osnovu stanja shodno analizi vibracija ležišta, i to upotrebom Procene parametara signala rotacionom invarijantnom metodom (ESPRIT) za detekciju oštećenja na ležištima indukcionog motora. Rezultati eksperimentalnih ispitivanja indukcionog motora od 3 kW, 50 Hz pokazuju efikasnost metode ESPRIT u otkrivanju nisko-amplitudnih harmonika karakterističnih za oštećenja ležišta.*

failures such as bearing faults /10, 11/. This monitoring is carried out through the spectral analysis of the vibration signal, enabling the tracking of the evolution of frequency components characteristic of the defect. Consequently, it becomes possible to ascertain the condition of various bearing components.

To detect bearing defects in the early stages of their occurrence, various signal processing methods have been developed, among which is spectral analysis using Fast Fourier Transform, commonly known as FFT /12, 13/. This method is one of the most significant and widely utilised techniques since the introduction of spectrum analysers. However, this technique does not yield reliable results when the number of acquired signal samples is limited, i.e., when the acquisition time is short, /14, 15/.

To address this issue, it is necessary to increase the signal acquisition duration, thereby increasing the number of samples. However, this approach is often impractical in reality, given that most spectrum analysers used in the industry have limitations in terms of signal acquisition, such as a predefined frequency range and a limited number of samples. These constraints make it challenging to distinguish closely spaced characteristic frequencies. Consequently, it is imperative to employ more advanced analytical methods capable

of separating harmonics that are very close, independent of the resolution of the measuring instrument.

For this purpose, parametric methods are developed in the field of signal processing, particularly in the context of spectral analysis, with the aim of distinguishing closely spaced frequency components [1, 16]. These methods, known as high-resolution methods, have numerous applications in various fields, particularly recently in the vibration analysis of rotating machinery [17, 18]. Furthermore, these methods rely on decomposing the covariance matrix of the analysed signal into eigenvalues and eigenvectors. The goal is to assess the spectral content of the signal by distinguishing the space of useful data, generated by sinusoids, from the noise space [19-22]. Among these techniques, we find the Multiple Signal Classification (MUSIC) method that exploits the noise space, and the Estimation of Signal Parameters via Rotational Invariance Techniques (ESPRIT) method based on signal space. The applications of these methods in the diagnosis of bearing faults are detailed in [12, 18, 23].

The aim of this article is to diagnose mechanical faults, particularly bearing faults in induction motors operating under constant load and speed conditions, by analysing the vibration signal using the ESPRIT technique. This method stands out for its high robustness against measurement noise and superior frequency resolution compared to conventional approaches. However, this method demands a significant computation time which can be a hindrance during real-time implementation. Nevertheless, the proposed solution to mitigate this computation time constraint and reduce memory space usage is to process only the frequency band where the signature of the fault is expected, considering that the frequency signature of the targeted fault is located in a known frequency range.

In this study, we analysed a vibration signal generated by a three-phase asynchronous motor using the ESPRIT method for bearing fault detection. The obtained results are promising, demonstrating the capability of this method to detect harmonics of very low amplitudes.

## BEARING FAULT CHARACTERISTIC FREQUENCIES

Ball bearings are the most commonly used in electrical machines. They consist of an outer ring, an inner ring, balls that facilitate the movement of both rings with minimal friction, and a cage that maintains a uniform distance between the balls. Figure 1 illustrates the geometry of a radial contact ball bearing.

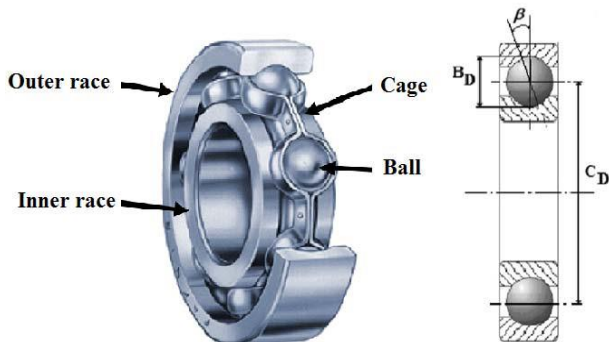


Figure 1. Geometry of a rolling-element bearing.

Furthermore, bearing faults manifest as specific harmonics in the vibration spectrum. The amplitudes and frequencies of these harmonics, dependent on bearing dimensions and shaft rotation frequency, allow for the characterisation of the bearing's condition. In this case, these frequencies are given as follows, [16, 24]:

$$\text{- outer race fault} \quad f_0 = \frac{N_b}{2} f_r \left( 1 - \frac{B_D}{C_D} \cos \beta \right), \quad (1)$$

$$\text{- inner race fault} \quad f_i = \frac{N_b}{2} f_r \left( 1 + \frac{B_D}{C_D} \cos \beta \right), \quad (2)$$

$$\text{- cage fault} \quad f_{cage} = \frac{1}{2} f_r \left( 1 - \frac{B_D}{C_D} \cos \beta \right), \quad (3)$$

$$\text{- ball fault:} \quad f_{ball} = \frac{C_D}{B_D} f_r \left( 1 - \frac{B_D^2}{C_D^2} \cos^2 \beta \right). \quad (4)$$

where:  $B_D$  and  $C_D$  are the balls and cage diameter, respectively;  $f_r$  is mechanical rotor frequency;  $N_b$  is the number of bearing balls; and  $\beta$ , is the contact angle.

## ESPRIT METHOD

The ESPRIT method was developed by Roy et al. [25]. This is a subspace estimation method in which parameter estimates (amplitude, frequency, and phase) of a sinusoidal signal are obtained by exploiting the rotational invariance structure of the signal subspace. We consider the following noisy sampled signal:

$$x(n) = \sum_{i=1}^L a_i \cos(2\pi f_i n T_s + \theta_i) + b(n) \quad ; \quad n=0,1,\dots,N, \quad (5)$$

where:  $a_i$ ,  $f_i$ , and  $\theta_i$  are respectively the amplitude, frequency and phase of the  $i$ -th sinusoidal component;  $b(n)$  is a measured noise that can be modelled as an additive white noise with a zero mean and a variance  $\sigma^2$ ;  $T_s$  is the sampling period;  $L$  is sinusoidal components number; and  $N$  is the acquired samples number.

According to Euler's formula, Eq.(5) can be written as follows:

$$x(n) = \sum_{i=1}^{2L} \frac{a_i e^{j\theta_i}}{2} e^{j2\pi f_i T_s n} + b(n) = \sum_{i=1}^{2L} A_i e^{j2\pi f_i T_s n} + b(n), \quad (6)$$

with  $A_i$ , the complex magnitudes.

In matrix form, Eq.(6) is written as, [26]:

$$X = SA + B, \quad (7)$$

where:  $X$ ,  $A$ , and  $B$  represent respectively the observation, amplitude, and noise vectors. They are defined as follows:

$$X = [x(n) \quad x(n+1) \quad \dots \quad x(n+m-1)]^T, \quad (8)$$

$$A = [A_1 \quad A_2 \quad \dots \quad A_{2L}]^T, \quad (9)$$

$$B = [b(n) \quad b(n+1) \quad \dots \quad b(n+m-1)]^T, \quad (10)$$

with  $S$  as the Vandermonde matrix,

$$S = [s_1 \quad s_2 \quad \dots \quad s_k \quad \dots \quad s_{2L}], \quad (11)$$

$$\text{where: } s_k = [1 \quad e^{j2\pi f_k T_s} \quad e^{j2\pi f_k 2T_s} \quad \dots \quad e^{j2\pi f_k (N-1)T_s}]^T. \quad (12)$$

## Frequency estimation

The signal frequencies estimation is based on the covariance matrix singular value decomposition of the noisy signal  $x(n)$ . This matrix is defined by the following relation:

$$Y = E[XX^H], \quad (13)$$

where:  $E[\cdot]$  is mathematical expectation; and  $H$  is the Hermitian transposition operator.

Additionally, this matrix can be considered as the sum of two covariance matrices, the signal and the noise matrix /27, 12/,

$$Y = Y_s + Y_b = S\Psi S^H + \sigma^2 I, \quad (14)$$

where:  $\Psi$  represents the power matrix of the sought harmonics, defined as follows:

$$\Psi = \text{diag}[A_1^2 \ A_2^2 \ \dots \ A_{2L}^2]. \quad (15)$$

In practice, the covariance matrix  $Y$  is unknown, however, it can be estimated from the following observations:

$$\hat{Y} = \frac{1}{N-m+1} \sum_{n=1}^{N-m+1} X(n)X(n)^H, \quad (16)$$

where:  $X = [x(n) \ x(n+1) \ \dots \ x(n+m-1)]^T$  is of length  $m$ .

The singular value decomposition allows the separation of the matrix  $Y$  into several orthogonal components according to the classification of singular values, /12/,

$$Y = \sum_{i=1}^{2L} \lambda_i u_i u_i^H + \sum_{i=2L+1}^N \lambda_i u_i u_i^H, \quad (17)$$

where:  $\lambda_i$  and  $u_i$  are respectively the eigenvalues and eigenvectors of matrix  $Y$ .

Thus, in matrix form, Eq.(17) is written

$$Y = U_s \Lambda_s U_s^H + U_b \Lambda_b U_b^H, \quad (18)$$

where:

$$U_s = [u_1, u_2, \dots, u_{2L}], \quad U_b = [u_{2L+1}, u_{2L+2}, \dots, u_N], \quad (19)$$

$$\Lambda_s = \text{diag}(\lambda_1, \lambda_2, \dots, \lambda_{2L}) \quad \Lambda_b = \sigma^2 I_{N-2L}, \quad (20)$$

with  $\Lambda_s$  as the matrix of signal space eigenvectors corresponding to the  $2L$  strongest eigenvalues;  $\Lambda_b$  is the noise space eigenvector matrix; and  $\sigma^2$  is the noise variance.

The ESPRIT method's main aspect is the property of the space signal's rotational invariance.

Then, two matrices  $S_1$  and  $S_2$  are defined as follows, /26, 28/:

$$S_1 = [I_{m-1} \ 0] S, \quad (21)$$

$$S_2 = [0 \ I_{m-1}] S, \quad (22)$$

where:  $S_1, S_2$  represent, respectively, the first and last rows of matrix  $S$ . with,  $I_{m-1}$  an identity matrix of dimension  $(m-1)(m-1)$ .

Subsequently, these two new matrices  $S_1$  and  $S_2$  are combined as shown in Eq.(23), which allows us to extract the eigenvalues /28/,

$$\Phi = (S_1^H S_1)^{-1} S_1^H S_2. \quad (23)$$

From this equation, the signal frequencies can be estimated using the following relation:

$$f_i = \frac{\arg(\Gamma_i)}{2\pi T_s}, \quad i=1, 2, \dots, L, \quad (24)$$

where:  $\Gamma_i$  are eigenvalues of the matrix  $\Phi$ .

#### Amplitudes and phases estimation

Once the signal frequencies are estimated, the complex amplitudes can then be determined using the least squares estimator. This estimator is given by /26, 29/:

$$C = (S^H S)^{-1} S^H X. \quad (25)$$

Finally, the initial amplitudes and phases can be obtained as follows:

$$a_i = 2|c_i|, \quad i=1, 2, \dots, L, \quad (26)$$

$$\theta_i = \arg(c_i), \quad i=1, 2, \dots, L, \quad (27)$$

where:  $c_i$  is the  $i$ -th component of  $c$ ;  $|\cdot|$  represents the complex module; and  $\arg(\cdot)$  argument.

#### Experimental results

The motor used in the experimental tests is a three-phase squirrel cage type, with nominal power of 3 kW, a frequency of 50 Hz, current of 7 A, and rotational speed of 1410 rpm. Additionally, this motor is mechanically coupled to a direct current generator connected to a resistive load. In addition, the measurement chain consists of an acquisition card and a piezoelectric-type accelerometer used to measure the vibrations of the motor. The entire setup is connected to a computer for visualisation and processing of recorded signals. Figure 2 illustrates the test bench used.



Figure 2. Photo of the test bench.

All acquisitions are performed under steady-state conditions, at constant load, over a duration of 20 seconds with a sampling frequency  $f_s = 10$  kHz. This ensures a frequency resolution of 0.05 Hz. Furthermore, the diagnosed bearings are of 6205-ZZ type, characterised by following parameters:  $N_b = 9$  balls,  $B_D = 7.938$  mm,  $C_D = 38.5$  mm, and  $\beta = 0$ . The fault addressed in this article concerns the outer ring and cage, as illustrated in Fig. 3.



Figure 3. Bearing faults: outer race fault (left); cage fault (right).

Furthermore, since various tests are conducted under a constant load at a speed of 1440 rpm, corresponding to a rotation frequency  $f_r = 24$  Hz, and based on the geometric parameters of the bearing and Eqs. (1) and (3), the vibration

signatures of bearing defects, if present, should manifest at the following theoretical frequencies, Table 1.

Table 1. Theoretical frequencies of bearing faults for  $f_r = 24$  Hz.

Bearing faults	Vibration frequency	The analysis band
outer race fault	85.73 Hz	[80 Hz, 90 Hz]
cage fault	9.52 Hz	[5 Hz, 15 Hz]

Table 1 demonstrates that analysing the spectrum of the vibration signal in specific frequency ranges around each characteristic fault frequency is adequate for detecting various bearing faults.

#### Healthy bearing

The measured vibration signal is shown in Fig. 4. It is noteworthy that this temporal waveform provides no information about the condition of the studied.

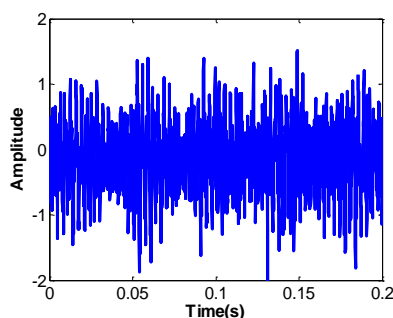


Figure 4. Vibration signal.

The spectral analysis of the vibration signal using FFT is shown in Fig. 5. This illustration reveals the presence of a component at the frequency of 85.85 Hz within the range [80 Hz, 90 Hz]. However, no frequency signatures are detected within the range [5 Hz, 15 Hz].

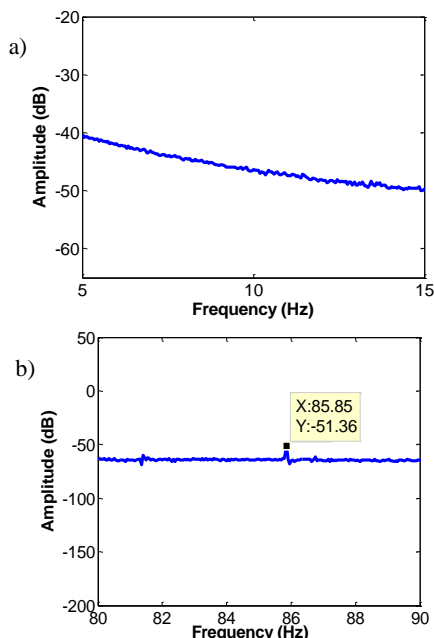


Figure 5. Vibration analysis by FFT algorithm: a) [5 Hz, 15 Hz]; b) [80 Hz, 90 Hz] - healthy bearing.

The application of the proposed ESPRIT method to the same frequency ranges mentioned above yield the following results.

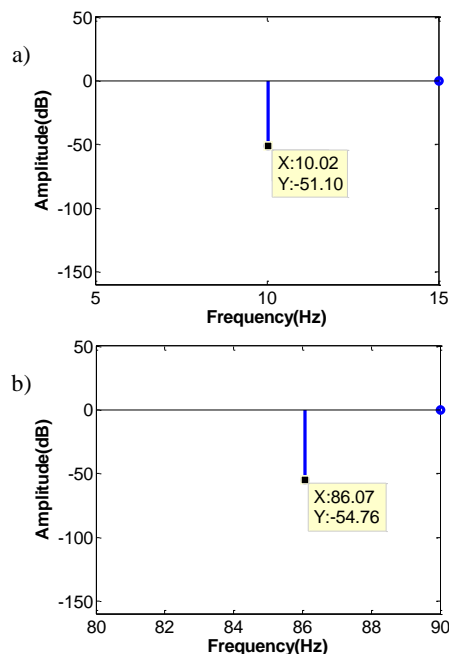


Figure 6. Vibration analysis by the ESPRIT algorithm: a) [5 Hz, 15 Hz]; b) [80 Hz, 90 Hz] - healthy bearing.

Figure 6 demonstrates that, in addition to the harmonic revealed at 86.07 Hz by both methods (FFT and ESPRIT), another harmonic appears at 10.02 Hz in the spectrum obtained by ESPRIT. This confirms its ability to identify low-amplitude harmonics compared to the conventional method.

Comparing this result with Table 1, we can speculate that these very low-amplitude harmonics might correspond to a minor scratch on the outer ring and cage of the bearing which should remain intact. Thus, this scratch could be explained by the repetitive process of disassembly and assembly of bearings during various tests (multiple tests with the same bearing). Therefore, this characteristic can be considered as an incipient defect.

Indeed, the signals acquired and analysed during this initial test will serve as a reference for all subsequent tests.

#### Bearing with an outer race fault

In this test, the motor operates with a bearing having a 3 mm hole in the outer ring. In this case, the theoretical characteristic frequency of this defect should appear at 85.73 Hz (see Table 1).

Figure 7 illustrates the vibration spectrum obtained by ESPRIT, highlighting the presence of a component at the frequency of 85.80 Hz.

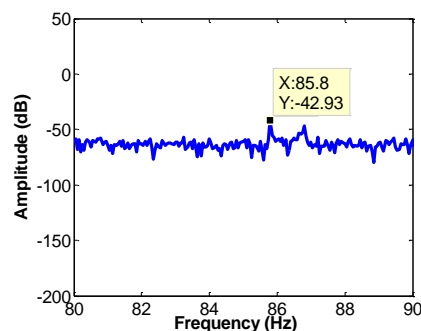


Figure 7. Vibration analysis by ESPRIT algorithm - outer race fault.



Figure 7 illustrates the presence of a harmonic at the frequency of 85.98 Hz, with a more significant amplitude compared to the case of the healthy bearing (Fig. 6b). This indicates a defect in the outer ring of the bearing.

#### Bearing with cage fault

In this test, a small hole is created in the bearing cage. Figure 8 shows the plot of the result obtained by FFT. Considering that, according to Table 1, the harmonic characterising this defect should appear at a frequency of 9.52 Hz. However, from this figure, it can be observed that the FFT fails to identify the frequency of the sought defect.

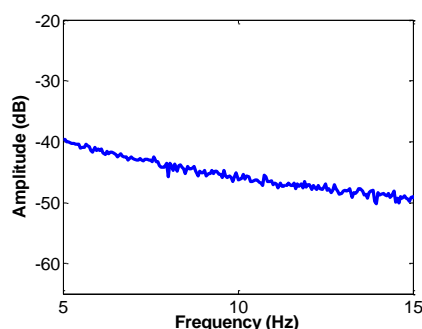


Figure 8. Vibration analysis by FFT algorithm - cage fault.

Analysing the vibration signal using the ESPRIT method yields the result illustrated in the following figure.

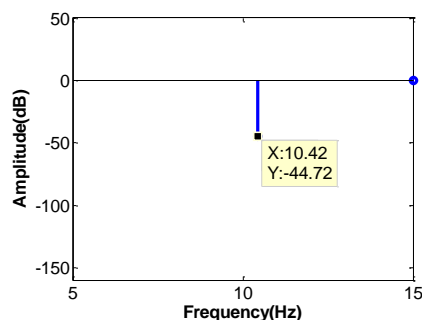


Figure 9. Vibration analysis by ESPRIT algorithm - cage fault.

According to Fig. 9, a component at a frequency of 10.42 Hz is observed with an increase in amplitude compared to the case where the bearing is healthy (Fig. 6a), indicating a sign of a defect in the cage.

Table 2 summarises and compares theoretical frequencies of the outer ring defect and cage defect with those obtained through the ESPRIT technique, along with the time taken by the latter.

Table 2. Theoretical and experimental values of faults harmonics (ESPRIT method).

Bearing fault	Theor. freq. (Hz)	Experimental results		
		Experimental frequency (Hz)	Analysis band	Computation time (s)
outer race fault	85.73	85.98	[0 Hz, $F_s/2$ ]	1146.1
			[80 Hz, 90Hz]	0.27
cage fault	9.52	10.42	[0 Hz, $F_s/2$ ]	1013.15
			[5 Hz, 15Hz]	0.24

According to Table 2, it is observed that results obtained by the ESPRIT algorithm are superior, as the frequencies identified by this method are very close to theoretical frequencies. Additionally, applying this method to well-defined

frequency ranges, where the defect is expected to appear leads to a significant reduction in computation time.

## CONCLUSION

This article proposes a reliable and effective ESPRIT technique for identifying mechanical faults, particularly bearing faults in induction motors by analysing the vibration signal. This approach overcomes the limitations and disadvantages of spectral resolution observed in the classical DSP method (FFT). Experimental results demonstrate the superiority of the proposed approach compared to the classical method in detecting certain frequency signatures of very low amplitude. Additionally, the ESPRIT method enables tracking the severity evolution of bearing faults. However, the ESPRIT algorithm has a high computation time. To alleviate this constraint, processing is focused on frequency bands where the sought fault signature is likely to appear. This strategy reduces computation time without compromising analysis precision, making the technique suitable for real-time applications.

## REFERENCES

1. Azouzi, K., Boudinar, A.H., Bendiabdellah, A. (2018), *Detection of bearing faults in induction motor by a combined approach SVD-Kalman filter*, Int. Rev. Autom. Control (IREA CO), 11(1): 14-22. doi: 10.15866/ireaco.v11i1.13501
2. Toma, R.N., Prosvirin, A.E., Kim, J.-M. (2020), *Bearing fault diagnosis of induction motors using a genetic algorithm and machine learning classifiers*, Sensors, 20(7): 1884. doi: 10.3390/s20071884
3. Singh, G., Kumar, T.C.A., Naikan, V.N.A. (2018), *A non intrusive methodology for bearing current detection in PWM inverter fed induction motor drive*, Int. Conf. on Power, Instrumentation, Control and Computing (PICC), Thrissur, India, 2018, pp.1-6. doi: 10.1109/PICC.2018.8384807
4. Barusu, M.R., Deivasigamani, M. (2020), *Non-invasive vibration measurement for diagnosis of bearing faults in 3-phase squirrel cage induction motor using microwave sensor*, IEEE Sensors J, 21(2): 1026-1039. doi: 10.1109/JSEN.2020.3004515
5. Maruthi, G.S., Hegde, V. (2015), *Application of MEMS accelerometer for detection and diagnosis of multiple faults in the roller element bearings of three phase induction motor*, IEEE Sensors J, 16(1): 145-152. doi: 10.1109/JSEN.2015.2476561
6. Fontes Godoy, W., Morinigo-Sotelo, D., Duque-Perez, O., et al. (2020), *Estimation of bearing fault severity in line-connected and inverter-fed three-phase induction motors*, Energies, 13(13): 3481. doi: 10.3390/en13133481
7. Bazan, G.H., Scalassara, P.R., Endo, W., Goedel, A. (2019), *Information theoretical measurements from induction motors under several load and voltage conditions for bearing faults classification*, IEEE Trans. Industr. Inform. 16(6): 3640-3650. doi: 10.1109/TII.2019.2939678
8. Nishat Toma, R., Kim, J.-M. (2020), *Bearing fault classification of induction motors using discrete wavelet transform and ensemble machine learning algorithms*, Applied Sciences, 10(15): 5251. doi: 10.3390/app10155251
9. Kumar, P., Hati, A.S. (2022), *Dilated convolutional neural network based model for bearing faults and broken rotor bar detection in squirrel cage induction motors*, Expert Syst. Appl. 191: 116290. doi: 10.1016/j.eswa.2021.116290
10. Chandra, D.S., Rao, Y.S. (2019), *Fault diagnosis of a double-row spherical roller bearing for induction motor using vibration monitoring technique*, J Fail. Anal. Prev. 19: 1144-1152. doi: 10.1007/s11668-019-00712-z

11. Saini, M.K., Aggarwal, A. (2018), *Detection and diagnosis of induction motor bearing faults using multiwavelet transform and naive Bayes classifier*, Int. Trans. Electr. Energ. Syst. 28(8): e2577. doi: 10.1002/etep.2577
12. Boudinar, A.H., Benouzza, N., Bendiabdellah, A., Khodja, M.E.A. (2016), *Induction motor bearing fault analysis using a root-MUSIC method*, IEEE Trans. Indust. Appl. 52(5): 3851-3860. doi: 10.1109/TIA.2016.2581143
13. Kompella, K.C.D., Rao Mannam, V.G., Rao Rayapudi, S. (2018), *Bearing fault detection in a 3 phase induction motor using stator current frequency spectral subtraction with various wavelet decomposition techniques*, Ain Shams Eng. J. 9(4): 2427-2439. doi: 10.1016/j.asej.2017.06.002
14. Azouzi, K., Boudinar, A.H., Aimer, F.A., Bendiabdellah, A. (2018), *Use of a combined SVD-Kalman filter approach for induction motor broken rotor bars identification*, J Microw. Optoelectron. Electromagn. Appl. 17(1): 85-101. doi: 10.1590/2179-10742018v17i11136
15. Kompella, K.C.D., Mannam, V.G.R., Rayapudi, S.R. (2016), *DWT based bearing fault detection in induction motor using noise cancellation*, J Electr. Syst. Inf. Technol. 3(3): 411-427. doi: 10.1016/j.jesit.2016.07.002
16. Elbouchikhi, E., Choqueuse, V., Benbouzid, M. (2016), *Induction machine bearing faults detection based on a multi-dimensional MUSIC algorithm and maximum likelihood estimation*, ISA Trans. 63: 413-424. doi: 10.1016/j.isatra.2016.03.007
17. Delgado-Arredondo, P.A., Garcia-Perez, A., Morinigo-Sotelo, D., et al. (2015), *Comparative study of time-frequency decomposition techniques for fault detection in induction motors using vibration analysis during startup transient*, Shock Vibr. 2015: 708034. doi: 10.1155/2015/708034
18. Agrawal, S., Mohanty, S.R., Agarwal, V. (2015), *Bearing fault detection using Hilbert and high frequency resolution techniques*, IETE J Res. 61(2): 99-108. doi: 10.1080/03772063.2015.1009398
19. Singh, G., Naikan, V.N.A. (2018), *Detection of half broken rotor bar fault in VFD driven induction motor drive using motor square current MUSIC analysis*, Mech. Syst. Signal Process. 110: 333-348. doi: 10.1016/j.ymssp.2018.03.001
20. Chakkor, S., Baghour, M., Hajraoui, A. (2015), *High accuracy ESPRIT-TLS technique for wind turbine fault discrimination*, Int. J Electr. Comp. Eng. 9(1): 122-131.
21. Xu, B., Sun, L., Xu, L., Xu, G. (2012), *An ESPRIT-SAA-based detection method for broken rotor bar fault in induction motors*, IEEE Trans. Ener. Convers. 27(3): 654-660. doi: 10.1109/TEC.2012.2194148
22. Kim, Y.-H., Youn, Y.-W., Hwang, D.-H., et al. (2012), *High-resolution parameter estimation method to identify broken rotor bar faults in induction motors*, IEEE Trans. Ind. Elec. 60(9): 4103-4117. doi: 10.1109/TIE.2012.2227912
23. Masmoudi, M.L., Etien, E., Moreau, S., Sakout, A. (2017), *Single point bearing fault diagnosis using simplified frequency model*, Electr. Eng. 99: 455-465. doi: 10.1007/s00202-016-0441-y
24. He, W., Zi, Y., Chen, B., et al. (2015), *Automatic fault feature extraction of mechanical anomaly on induction motor bearing using ensemble super-wavelet transform*, Mech. Syst. Signal Process. 54-55: 457-480. doi: 10.1016/j.ymssp.2014.09.007
25. Roy, R., Paulraj, A., Kailath, T. (1986), *ESPRIT-A subspace rotation approach to estimation of parameters of cisoids in noise*, IEEE Trans. Acoust., Speech, Signal Process. 34(5): 1340-1342. doi: 10.1109/TASSP.1986.1164935
26. Trachi, Y., Elbouchikhi, E., Choqueuse, V., Benbouzid, M.E.H. (2016), *Induction machines fault detection based on subspace spectral estimation*, IEEE Trans. Industr. Electr. 63(9): 5641-5651. doi: 10.1109/TIE.2016.2570741
27. Elbouchikhi, E., Choqueuse, V.V., Benbouzid, M. (2015), *Induction machine diagnosis using stator current advanced signal processing*, Int. J Energy Convers. 3(3): 76-87.
28. Alfieri, L., Carpinelli, G., Bracale, A. (2015), *New ESPRIT-based method for an efficient assessment of waveform distortions in power systems*, Elec. Pow. Syst. Res. 122: 130-139. doi: 10.1016/j.epsr.2015.01.011
29. Xu, B., Sun, L., Xu, L., Xu, G. (2013), *Improvement of the Hilbert method via ESPRIT for detecting rotor fault in induction motors at low slip*, IEEE Trans. Energy Convers. 28(1): 225-233. doi: 10.1109/TEC.2012.2236557

© 2025 The Author. Structural Integrity and Life, Published by DIVK (The Society for Structural Integrity and Life 'Prof. Dr Stojan Sedmak') (<http://divk.inovacionicentar.rs/ivk/home.html>). This is an open access article distributed under the terms and conditions of the Creative Commons Attribution-NonCommercial-NoDerivatives 4.0 International License